06

Configuration and dynamics of vortex lines of three-dimensional vector laser toroidal solitons

© N.A. Veretenov, N.N. Rosanov, S.V. Fedorov

Ioffe Institute, St. Petersburg, Russia

e-mail: torrek@gmail.com, nnrosanov@mail.ru, sfedorov2006@bk.ru

Received June 21, 2023
Revised July 23, 2023
Accepted October 30, 2023.

A wide class of toroidal three-dimensional dissipative vector solitons in a medium containing centers with nonlinear laser amplification and absorption has been found numerically. The structure and dynamics of the topological singularities of these solitons are analyzed.

Keywords: three-dimensional dissipative optical solitons, vector solitons, topological singularities.

DOI: 10.61011/EOS.2023.11.58029.5344-23

Multidimensional dissipative optical solitons attract attention both due to their general scientific interest and the prospects for localizing energy in them and the opportunity of volumetric recording and processing of information, see recent monographs [1–3], reviews [4–6] and references therein.

The topic of optical solitons under study intersects with the section of singular or topological optics [7–9]. For quasi-monochromatic paraxial wave packets, solitons can have phase and polarization singularities. The first ones correspond to the uncertainty of the phase of any transverse component of the electric field. They are characterized by an integer topological index m. This index is defined as the phase increment of a component as it moves around a closed loop around the singularity point at which the amplitude vanishes, divided by 2π. The circuit is located in a plane orthogonal to the direction of radiation propagation. Polarization singularities correspond to the uncertainty of the polarization state. Their half-integer index η (Poincare index) is equal to the angle of rotation of the polarization ellipse when going around the singular point, divided by 2π.

In a linear homogeneous medium, singularities of higher orders turn out to be unstable, and the structure with the topological charge $m > 1$ breaks up into fragments m with unit charges [7,10]. The same disintegration occurs in a medium with Kerr nonlinearity [11]. The situation changes in the case of nonlinear dissipative media. In [12] stable scalar two-dimensional laser solitons with topological charges $m = 1$, 2 and 3 were found. In $3D$-geometry, singularities are formed by lines and surfaces, see [2,5] and references therein. The stability regions narrow sharply with increasing m. The situation changes for vector (polarization) solitons due to the mutual support of polarization components [13].

In the work [6] $3D$-toroidal vector solitons with polarization singularities were found. In this work we will pay attention to the structure and dynamics of such solitons.

Model and master equation

In the quasi-optical approximation, the electrical intensity envelope has only transverse Cartesian $E_\wedge = (E_x, E_y)$ or circular $E_\pm = \frac{1}{\sqrt{2}}(E_x \pm iE_y)$ components (x and y — transverse coordinates) [6]. The medium consists of a matrix with linear characteristics doped with centers with nonlinear enhancement and absorption. For passive centers we use a model of a medium with two levels [14], and for active centers — a 4-level model with a spin flip [15], which is adopted for semiconductor lasers. In the accompanying coordinate system $(x, y, z, \tau = t - z/v_{gr})$, where z — longitudinal coordinate, t — time and v_{gr} group velocity, the dimensionless control equation for the envelopes of circular polarization components under the restrictions specified in [6] looks like

$$\frac{\partial E_\pm}{\partial z} = (i + d)\Big(\frac{\partial^2}{\partial x^2} + \frac{\partial^2}{\partial y^2} + \frac{\partial^2}{\partial \tau^2}\Big)E_\pm + f_\pm(I, \delta I)E_\pm, \tag{1}$$

where the nonlinear function $f_\pm$ is given by

$$f_\pm = f_\pm(I, dl) = -1 - \frac{a_0}{1+I} + \frac{g_0}{1+b_gI}\Big|1 \pm \frac{e_Jb_gdI}{1+e_Jb_gdI}\Big| \times \Big|1 - \frac{e_Jb_g^2dI^2}{(1+b_gI)(1+e_Jb_gdI)}\Big|. \tag{2}$$

The meaning of the parameters included in (2) is explained in [6,13]. In the calculations, we varied the linear gain g_0, the diffusion constant$d$, and the ratio of the relaxation rate in active centers to the beat decay rate ε_J.

The steady-state structure of the field depends on the initial conditions. The envelopes of the polarization components were specified in the form of torus-shaped distributions with various combinations of topological charges m. At $z = 0$ the envelope looked like

$$E_\pm(x, y, \tau) = 3.1\exp(-(p/p_0)^2)\exp(im_\pm j), \tag{3}$$

Summary table of found toroidal solitons with charges of circular components up to $|m| = 7$

№	m_+	m_-	e_J	Polarization features
1	1	0	0.04	*C*-line, cylindrically symmetrical *L*-surface
2	1	−1	0	*V*-line, linear to polarization
3	2	−1	0.04	*V*-line, cylindrically symmetrical *L*-surface
4	3	−1	0.04	*V*-line, *L*-surface
5	2	−2	0.04	*V*-line, linear to polarization
6	3	−2	0.04	3
7	3	−3	0.04	*V*-line, linear to polarization
8	4	−2	0.04	6 *C*-lines, *L*-surfaces
9	4	−3	0.08	7 *C*-lines, *L*-surfaces
10	4	−4	0.1	4 *V*-lines, *L*-surfaces
11	5	−5	0.1	1 *V*-lines, 8 *C*lines, *L*-surfaces
12	5	−1	0.12	1 *V*-lines, 2 double *C*-lines, *L* -surfaces
13	6	−1	0.06	7 *C*-lines, *L*-surfaces
14	7	−1	0.08	8 *C*-lines, *L*-surfaces
15	7	−5	0.12	1 *V*-lines, 12 *C*lines, *L*-surfaces

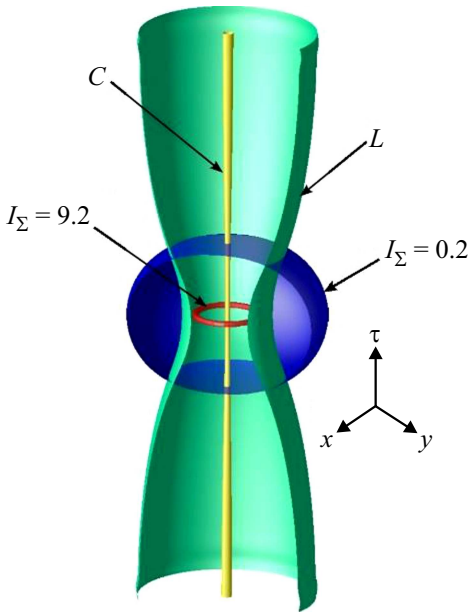

Figure 1. Soliton isosurfaces (1,0) by total intensity levels 0.2 (blue surface) and 9.2 (red ring) and special elements: *C*-line (yellow) and cylindrically symmetrical *L*-surface (green).

$$r = \sqrt{x^2 + y^2}, \quad R = \sqrt{x^2 + y^2 + \tau^2},$$
$$j = \arctan(y/x), \quad Q = \arctan(r/\tau), \qquad (4)$$
$$p = \sqrt{R^2 + R_0^2 - 2rR_0 \sin(Q)}.$$

Profile width p_0 took values from 2 to 6. The radius of the torus R_0 was taken in the range from 10 to 12. The signs of topological charges do not affect the stability and intensity distribution of the soliton.

Simulation results

The Crank-Nicholson method was used for the linear step, the Euler method was used for the nonlinear step. The size of the step in space is $dx = dy = d\tau = 0.3 - 0.8$, in the evolutionary variable is $dz = 0.005 - 0.15$. Boundary conditions —$\partial E/\partial x = \partial E/\partial y = \partial E/\partial \tau = 0$.

A summary of information on stable solitons with topological charges $m_\pm$ from 0 to 7 is given in the table. Singularities correspond to *V*-lines on which the field turns to 0, *C*-lines where the polarization is circular, and *L*-surfaces with linear polarization. The multiple vortex line of each of the polarization components with charge $m_\pm$ during evolution can decay into $|m_\pm|$ vortex lines with $|m| = 1$. The Poincare index η was determined in the plane passing through the center of the soliton perpendicular to the axis t. For single vortex lines the index is $\eta = \pm 1/2$, for multiple lines the indices of the component lines are summed up. It is convenient to define the integral Poincare index when the traversal circuit covers all singularities. Its value equals: $\eta = (m_+ - m_-/2)$.

The table contains a column e_J. If its value is higher than the „standard “, $e_J = 0.004$, this is the threshold value from which this soliton is stable. Solitons up to $m = 4$ have

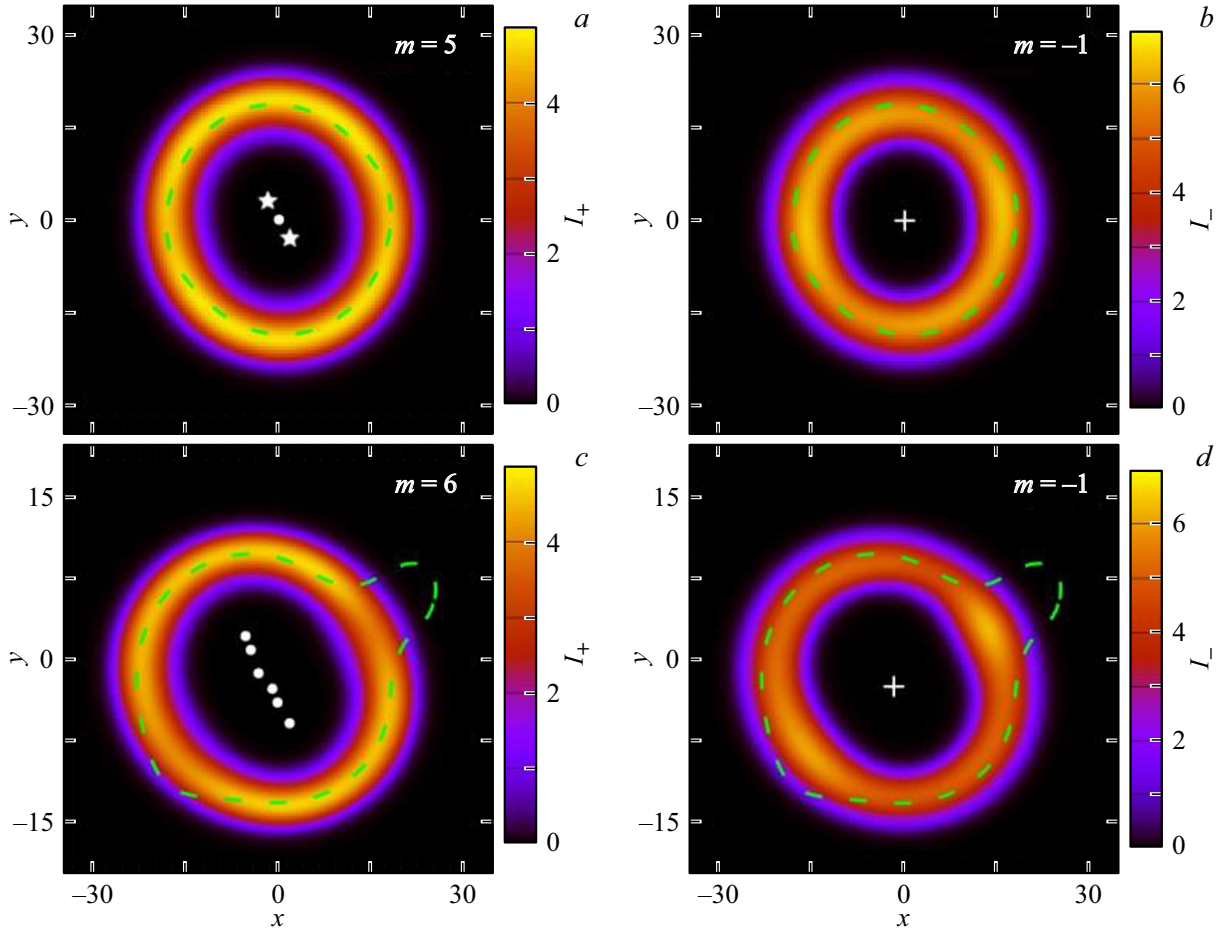

Figure 2. Transverse intensity distribution of stable toroidal solitons with charges of circular components $m_+ = 5$, $m_- = -1$ (top row, a, b) and $m_+ = 6$, $m_- = -1$ (bottom row, c, d). The intensity distribution of circular components is shown in a section passing perpendicular to the τ axis approximately through the center of the soliton. White dots (crosses) indicate the positions of vortex lines with charge 1 (-1), and dotted green lines indicate sections — of L surfaces. White stars correspond to the position of two merged vortex lines. Parameters: $g_0 = 2.14$, $d = 0.08$, $z = 10^4$, $e_J = 0.12$ (a, b), $e_J = 0.08$ (c, d).

a plane of symmetry of the intensity distribution, passing through the center of the soliton perpendicular to the t axis. Solitons (1,0) and (1,-1) are cylindrically symmetric. The vortex lines near the soliton center coincide, and far from the center they diverge due to noise, while this is practically not reflected in the intensity profile for solitons with the maximum charge of the $|m|_{\max} < 3$ components. A noticeable shift from symmetry occurs in the (4,-2) soliton, which has a 2nd order axis and rotates around this axis. With $|m|_{\max} > 3$, the vortex lines diverge, and C- or V-lines appear.

The simplest soliton with polarization features has components with charges 1 and 0. It exists in the high-pumping region of $g_0 = 2.15$. The soliton is cylindrically symmetrical, motionless, and the vortex line of the positive component is a straight C-line surrounded by an L-surface. On the soliton axis the intensity decreases, but does not reach zero. The soliton is at rest in a reference frame moving with group velocity.

Figure 1 shows isosurfaces of the total soliton intensity (1,0) and special elements: C-line, L-surfaces. For other solitons in the table we present a cross section in the (x, y) plane passing through the center of the soliton perpendicular to the τ axis.

Let us give some examples. The structure of the (5,-1) soliton in the (x, y) plane passing through its center is shown in Fig. 2, top row. The intensity distribution (as well as special elements of the polarization structure) has a second-order symmetry axis, is rigid, and rotates around its axis with a constant angular velocity. The center of the soliton on the (x, y) plane is inactive. Such a soliton contains 2C-lines („double“, with a Poincars index equal to 1, and marked as asterisks) and one straight V-line. The soliton (6,-1), shown in Fig. 2 in the bottom row, rotates and pulsates, while the center of the soliton in the (x, y) plane moves along a quasiperiodic trajectory. The soliton (6,-1) contains 7C-lines, since the only vortex line of the component E_+ does not coincide at any z with one specific of the six lines E_-, but alternately approaches one of them.

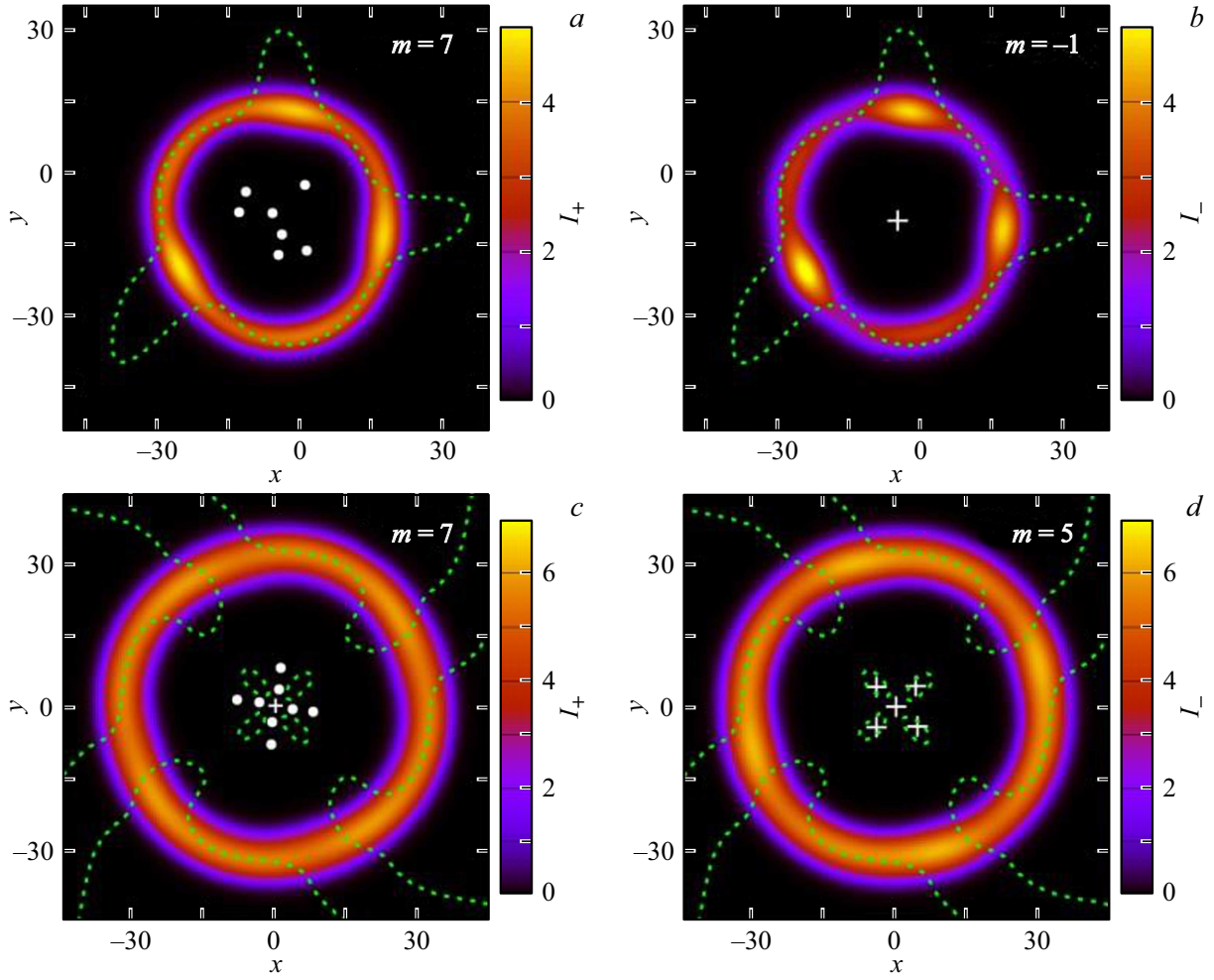

Figure 3. The same as in Fig. 2, for stable toroidal solitons with charges of circular components $m_+ = 7$, $m_- = -1$ (top row) and $m_+ = 7$, $m_- = -5$ (bottom row). The position of the central vortex line of the E_+ component, oriented opposite to the others, is indicated in the bottom left quadrant. The bottom row shows the intensities of the positive (left) and negative (right) circular components in a section passing perpendicular to the τ axis approximately through the center of the soliton. White dots (crosses) indicate the positions of vortex lines with charge 1 (-1), and dotted green lines indicate — sections of L surfaces. Parameters: $g_0 = 2.138$, $d = 0.09$, $e_J = 0.08$, $z = 10^4$ (a, b), $g_0 = 2.144$, $d = 0.09$, $e_J = 0.12$, $z = 10^4$ $(c,\ d)$.

When the parameter e_J increases to 0.08, the movement becomes chaotic.

The soliton (7,-1), shown in Fig. 3 (top row), rotates and oscillates chaotically, the position of the vortex lines changes. The soliton center in the (x, y) plane moves randomly. The only vortex line of the component E_- does not constantly coincide with any of the 7 lines E_+, the soliton is asymmetric. The bottom row of Fig. 3 shows the circular components of the soliton (7,-5), which is a rigid structure with a constant location of the vortex lines of both components. In this case, the total topological charge of the component has not changed and is equal to 7. The central vortex lines of both components are straight and coincide (V line). The soliton rotates like a rigid body and has a 4th order symmetry axis. In total, the soliton contains 8 C-lines and 1 V-line with a Poincare charge equal to 1.

Conclusion

The results confirm that vector laser solitons are much more stable than scalar ones due to the mutual support of polarization components. The existence of toroidal solitons with different polarization features is predicted. The stability of solitons with higher-order singularities depends on the type of nonlinearity. In the 4-level model, the critical parameter is e_J, determined by the relaxation characteristics of the amplifying medium. The symmetry of solitons and the dynamics of vortex lines of circular components also depend on the parameter e_J. The ratio of topological charges affects the topology of the soliton. If the vortex lines are located symmetrically, the stability of the soliton is higher, and the threshold value e_J is lower. The polarization components can produce a pair of vortex lines with the opposite sign of the topological charge. In this case, the

total charge is conserved, and the order of symmetry of the soliton increases. This occurs in the region of low intensities in the central region of the soliton.

Acknowledgments

This study was supported by the Russian Science Foundation under grant № 23-12-00012. The study results were obtained using the computing resources of the supercomputing center of Peter the Great St. Petersburg Polytechnic University (www.spbstu.ru).

Conflict of interest

The authors declare that they have no conflict of interest

References

[1] B.A. Malomed. *Multidimensional Solitons* (AIP, Melville, NY., 2022).
[2] N.N. Rozanov. *Dissipativnyye opticheskiye i rodstvennyye solitony* (Fizmatlit, M., 2021) (in Russian).
[3] M.F.S. Ferreira (ed.). *Dissipative Optical Solitons*, **238** (Springer Series in Optical Sciences, Cham, Switzerland, 2022).
[4] B.A. Malomed. Chaos, Solitons Fractals, **163**, 112526 (2022). DOI: 10.1016/j.chaos.2022.112526
[5] N.A. Veretenov, N.N. Rozanov, S.V. Fedorov. Uspekhi fiz. nauk, **192** (2), 143–176 (2022) (in Russian). DOI: 10.3367/UFNr.2020.11.038869 [N.A. Veretenov, N.N. Rosanov, S.V. Fedorov. Phys.-Usp. **65**, 131 (2022). DOI: 10.3367/UFNe.2020.11.038869].
[6] N.A. Veretenov, N.N. Rozanov, S.V. Fedorov. Izv. vuzov. Radiofizika. **66** (5–6), 447–460 (2023) (in Russian). DOI: 10.52452/00213462_2023_66_05_447
[7] M.S. Soskin, M.V. Vasnetsov. Prog. Opt., **42**, 219–276 (2001). DOI: 10.1016/S0079-6638(01)80018-4
[8] M.R. Dennis, K. O'Holleran, M.J. Padgett. Prog. Opt., **53**, 293–363 (2009). DOI: /10.1016/S0079-6638(08)00205-9
[9] D.S. Simon. *Topology in Optics: Tying Light in Knots* (IOP Publishing, Bristol, England, 2021).
[10] N.B. Baranova, B.Ya. Zeldovich. ZhETF **80** (5), 1789–1793 (1981) (in Russian).
[11] V.I. Kruglov, Yu.A. Logvin, V.M. Volkov. J. Mod. Opt., **39**, P. 2277–2291 (1992). DOI: 10.1080/09500349214552301
[12] S.V. Fedorov, N.N. Rosanov, A.N. Shatsev, N.A. Veretenov, A.G. Vladimirov. IEEE J. Quantum Electron., **39** (2), 197–205 (2003). DOI: 10.1109/JQE.2002.807212
[13] N.A. Veretenov, S.V. Fedorov, N.N. Rosanov. Phys. Rev. A, **107**, 013512 (2023). DOI: 10.1103/PhysRevA.107.013512
[14] N.N. Rozanov, S.V. Fedorov. Opt. i spektr., **72** (6), 1394–1399 (1992) (in Russian).
[15] M. San Miguel, Q. Feng, J.V. Moloney. Phys. Rev. A, **52**, 1728 (1995). DOI: 10.1103/PhysRevA.52.1728

Translated by E.Potapova